

without activation. Dissociation of the pair would involve reverse electron transfer to regenerate the carbene and alcohol molecules (if it occurred at all). In such a case, no electron-transfer intermediates should be experimentally discernible.

The direct reaction (Scheme III) of methanol with I leads to an intermediate triplet oxygen ylide of structure V. This species is calculated to be 15.8 kcal/mol less stable than the separated species, I and methanol. As a comparison, the corresponding ylide formed from methylene and methanol is predicted to be 1.9 kcal more stable than the separated species. These results suggest that the triplet state oxygen ylide is not an intermediate for this reaction. Turro has reported evidence for the reversible formation of an intermediate, presumed to be an ylide, in the reaction of I with alcohols.<sup>17</sup> It is possible that this intermediate be the radical ion pair of Scheme II.

The most plausible mechanism that does not involve thermal population of the carbene singlet state appears to be the electron-transfer mechanism (Scheme II). This suggestion is consistent with the reports that I reacts with amines<sup>18</sup> and carbon tetrachloride,<sup>19</sup> as one would expect

both to participate in electron-transfer reactions at least as well as alcohols. The intervention of the singlet state or an ylide cannot be rigorously ruled out by these calculations. Nevertheless, the activation energies required by the calculated reaction paths for Schemes I and III are beyond the normal errors expected for calculations of the kind presented in this paper.

While it is clear that the calculations reported in this paper cannot approach the level previously achieved for CH<sub>2</sub>, they can, nevertheless, provide the insight necessary for designing new and (hopefully) better experiments. In particular, the postulated mechanism can be tested. We do not mean to assert that the calculations prove the mechanism or disprove the suggestion that thermal excitation to the singlet is possible. However, these are the best calculations that can be done currently, and (with appropriate reservations) they certainly do not support the thermal excitation model. We hope these calculations will encourage further thinking in this area.

**Acknowledgment.** This work was supported in part by grants from the U.S.-Spain Cooperative Research Program, "Comision Asesora de Investigacion Cientifica y Technia" (PB85-0244) and The PSC-BHE.

(17) Turro, N. J.; Yuan, C.; Gould, I. R. *Tetrahedron Lett.* **1985**, 26, 5951.

(18) Nazran, A. S.; Griller, D. J. *Am. Chem. Soc.* **1985**, 107, 4613.

(19) Barcus, R. L.; Platz, M. S.; Scaiano, J. C. *J. Phys. Chem.* **1987**, 91, 695.

## Ab Initio Study of the Regiochemistry of Dimetalated Oximes. The Importance of Triple Ions in Isomeric Lithium and Sodium Ion Pairs of the Acetaldoxime Dianion

Rainer Glaser<sup>1</sup> and Andrew Streitwieser\*

*Department of Chemistry, University of California, Berkeley, California 94720*

*Received July 20, 1988*

The potential energy surfaces of dilithioacetaldoxime and its sodium analogue have been explored at the ab initio level. Several stationary points have been located with a slightly modified 3-21+G basis set. Harmonic vibrational frequencies have been calculated to characterize the stationary points, and energies have been obtained with a slightly modified 6-31+G\* basis set. The relative energies of the isomeric dimetalated derivatives of acetaldoxime show a preference for the formation of the syn-configured isomer, whereas in the case of the isolated dianion the anti isomer is thermodynamically favored by 2.2 kcal mol<sup>-1</sup>. The relative energies of the isomeric metal derivatives of acetaldoxime are in agreement with experiment. The regioselective second deprotonation at the syn  $\alpha$ -carbon and the regioselective addition of electrophiles to the syn  $\alpha$ -carbon are consistent with the calculated structures of the dimetalated intermediates. These results suggest that these structures of dimetalated oximes be considered in discussions of reaction mechanism. Triple ions formed by the heteroatoms and the cations are the primary structural concept. Chelation by the heteroatoms is more important than the interaction of the cations with the (formally) carbanionic methylene group. The triple ions formed between the heteroatoms and the cations differ in detail due to modes of puckering and give rise to topologically different structures. The syn preference energy for the dilithium derivatives of acetaldoxime is 4.4 kcal mol<sup>-1</sup>. Sodium increases the syn preference energy to 8.3 kcal mol<sup>-1</sup> and suggests that larger regioselectivity may be possible by use of bases with large cations. The interactions between sodium and the heteroatoms, nitrogen in particular, are enhanced compared to lithium. Replacement of Li<sup>+</sup> by Na<sup>+</sup> results in structures of different topology in some cases.

### Introduction

The regioselective formation of a new CC bond in the  $\alpha$ -position of a carbonyl group is one of the fundamental reactions in modern synthetic organic chemistry.<sup>2</sup> Di-

metalated oximes<sup>3-12</sup> and a variety of other N derivatives<sup>13</sup> of carbonyl compounds have been successfully employed

(3) Henoch, F. E.; Hampton, K. G.; Hauser, C. R. *J. Am. Chem. Soc.* **1969**, 91, 676.

(4) Beam, C. F.; Dyer, M. C. D.; Schwarz, R. A.; Hauser, C. R. *J. Org. Chem.* **1970**, 35, 1806.

(5) Jung, M. E.; Blair, P. A.; Lowe, J. A. *Tetrahedron Lett.* **1976**, 1439.

(6) Kofron, W. G.; Yeh, M.-K. *J. Org. Chem.* **1976**, 41, 439.

(7) Lyle, R. E.; Saavedra, J. E.; Lyle, G. G.; Fribush, H. M.; Marshall, J. L.; Lijinskij, W.; Singer, G. M. *Tetrahedron Lett.* **1976**, 4431.

(1) Predoctoral Fellow of the Fonds der Chemischen Industrie, 1985-87. Present address: Department of Chemistry, University of Missouri-Columbia, College Ave., Columbia, MO 65211.

(2) House, H. O. *Modern Synthetic Reactions*, 2nd ed.; The Benjamin/Cummings Publishing Co.: Menlo Park, CA, 1972.

**Table I. Energies and Vibrational Zero-Point Energies of the Isomeric Acetaldoxime Dianions and Their Lithium and Sodium Derivatives**

molecule	rel energies <sup>f</sup>							
	3-21+G <sup>a</sup>	6-31+G** <sup>a</sup>	ZPE <sup>b</sup>	CSP <sup>c</sup>	3-21+G		6-31+G*	
					SCF	SCF+ZPE	SCF	SCF+ZPE
1, C <sub>s</sub>	205.359 381	206.455 991	29.66	M	2.98	2.36	2.77	2.15
2, C <sub>1</sub>	205.364 134	206.460 411	29.28	M	0.00	0.00	0.00	0.00
3, C <sub>s</sub>	205.363 908	206.458 499	28.97	TS	0.14	-0.14	1.20	0.92
4, C <sub>1</sub>	220.494 806	221.677 705	35.64	M	0.00	0.00	0.00	0.00
5, C <sub>s</sub>	220.494 703	221.675 065	35.76	M	0.06	-0.12	1.66	1.48
6, C <sub>s</sub>	220.480 740	221.669 186	34.54	TS	8.83	7.55	5.35	4.07
7, C <sub>s</sub>	220.455 978	221.653 087	34.36	TS	24.36	22.92	15.45	14.01
8, C <sub>s</sub>	220.490 515	221.669 994	35.46	M	2.69	2.24	4.84	4.39
9, C <sub>1</sub>	220.446 147	221.635 994	34.76	M	30.53	29.45	26.17	25.09
10, C <sub>s</sub>	527.408 579	530.418 915	34.43	M	0.00	0.00	0.00	0.00
11, C <sub>1</sub>	527.408 328	530.418 013	34.40	M <sup>d</sup>	0.16	0.13	0.56	0.53
12, C <sub>s</sub>	527.399 902	530.404 796	33.83	TS <sup>e</sup>	5.44	4.90	8.86	8.32
13, C <sub>1</sub>	527.402 559	530.402 791	34.26	M <sup>e</sup>	3.78	3.63	10.12	9.98

<sup>a</sup>Total energies ( $-E$ , in atomic units) based on the RHF/3-21+G structures. No d functions and no diffuse functions on Li<sup>+</sup> and Na<sup>+</sup>, see text. <sup>b</sup>Unscaled. <sup>c</sup>Character of the stationary point: M = minimum, TS = transition state structure. <sup>d</sup>See ref 50. <sup>e</sup>See text for discussion of basis set effects. <sup>f</sup>Vibrational zero-point energy corrections to relative energies (in kcal/mol) are scaled (factor 0.9).

for this purpose. Dimetalations of oximes were first demonstrated by Hauser et al.<sup>3,4</sup> Treatment of acetophenone oxime with butyllithium in THF has been shown to give a stable dilithioacetophenone oxime. The dimetalated enolate equivalent can be alkylated, and reaction with 2,3-dibromo-2,3-dimethylbutane results in dimerization comparable to the oxidative coupling of metalated oxime ethers.<sup>14</sup> The formation of 1,6-diketoximes by 2-fold alkylation with 1,4-dibromobutane provides a simple method for the preparation of substituted 1,6-dicarbonyl compounds. Simultaneous studies by Jung et al.<sup>5</sup> and by Kofron and Yeh<sup>6</sup> have established that reactions of dimetalated oximes with electrophiles proceed regioselectively via the syn-configured intermediate, that is, the dimetalated oxime in which the deprotonated carbon and the oxygen are cis with respect to the NC bond. Methylation of dilithioacetaldoxime results exclusively in the formation of the lithium salt of the (*Z*)-oxime. Regeneration of the dilithium derivative and a second alkylation results in the  $\alpha,\alpha$ -dialkylated (*Z*)-oxime. The relatively higher stability of the syn-configured intermediate compensates for the formation of the secondary carbanion compared to the generally preferred formation of the primary carbanion. This regioselective alkylation provides an excellent method for the stereoselective synthesis of thermodynamically less favored oxime isomers that upon heating can be converted to the thermodynamically favored isomer. Lyle et al.<sup>7</sup> have studied the methylation of 4-*tert*-butylcyclohexanone oxime and have found that *trans*-2-methyl-4-*tert*-butylcyclohexanone oxime is produced exclusively. Alkylation of the dimetalated derivatives of cyclic ketoximes thus proceeds via chair-type transition states and results stereospecifically in syn-axial

alkylation. The observed regioselective formation of the syn-configured intermediate does not require any regioselectivity of the proton abstraction but only facile syn/anti isomerization of the intermediate. If the deprotonation were regioselective, two alternative pathways could account for the regioselective alkylation: regioselective deprotonation and subsequent alkylation at the syn  $\alpha$ -carbon (path A) or regioselective deprotonation of the anti  $\alpha$ -carbon followed by syn/anti isomerization and syn alkylation (path B). Lyle et al.<sup>8</sup> have studied the stereochemistry of the methylation of the single geometrical enantiomeric isomer (*Z*)-(2*R*,6*S*)-(+)-1-methyl-2,6-diphenyl-4-piperidone oxime. Methylation resulted in only the formation of optically pure (*Z*)-(2*R*,3*S*,6*S*)-1,3-dimethyl-2,6-diphenyl-4-piperidone, thus providing clear evidence that deprotonation and alkylation of oximes occur regioselectively at the syn  $\alpha$ -carbon.

While the stereochemistry of the formation of dimetalated oximes and of the reaction of electrophiles with such enolate equivalents has been well established, little is known about the structure of the metalated intermediates, and the factors causing the stereospecificity are open to dispute. It has generally been assumed on the basis of the Hammond postulate that the formation of the metalated intermediate under kinetic conditions leads to the kinetically and thermodynamically favored syn-configured intermediate. Jung et al.<sup>5</sup> and Lyle et al.<sup>7</sup> have argued that the regioselectivity originates primarily from additional stabilization of the syn dianion by through-space nonbonded interaction.<sup>15</sup> Such homoconjugation has been regarded as the reason for the remarkable stability of the syn-configured intermediate<sup>16</sup> as well as for the fact that no syn/anti isomerization occurs even after several hours.<sup>5</sup> On the other hand, Kofron and Yeh<sup>6</sup> have argued that chelation plays an important role for the stereospecific formation of the metalated intermediate. A 1,4-(C,O)- $\sigma$ -bridged structure in which the second metal cation coordinates solely to the oxygen atom has been proposed. It has been suggested that this type of chelation causes the

(8) Lyle, R. E.; Fribush, H. M.; Lyle, G. G.; Saavedra, J. E. *J. Org. Chem.* 1978, 43, 1275.

(9) Gawley, R. E.; Nagy, T. *Tetrahedron Lett.* 1984, 25, 263.

(10) Bellasoued, M.; Dardoize, F.; Frangin, Y.; Gaudemar, M. *J. Organomet. Chem.* 1979, 165, 1.

(11) Hassner, A.; Nümann, F. *Chem. Ber.* 1988, 121, 1823.

(12) Dimetalated oximes are presumably intermediates in the LAH reduction of dibenzyl oximes, which has been shown to proceed with high regioselectivity since a single aziridine is formed as the primary reduction product. Philips, J. C.; Perianayagam, C. *Tetrahedron Lett.* 1975, 7, 3263.

(13) Reviews: (a) Hickmott, P. W. *Tetrahedron* 1982, 14, 1975. (b) Enders, D. Alkylation of Chiral Hydrazones. In Morrison, J. D. *Asymmetric Synthesis*; Academic Press: New York, 1984; Vol. 3; p 275. (c) Seebach, D.; Geiss, K.-H. New Applications of Organometallic Reagents in Organic Synthesis. In Seyferth, D. *Journal of Organometallic Chemistry Library 1*; Elsevier Scientific Publishing Co.: Amsterdam, 1976.

(14) Shatzmiller, S.; Lidor, R. *Synthesis* 1983, 590.

(15) (a) Hoffmann, R.; Olofson, R. A. *J. Am. Chem. Soc.* 1966, 88, 943.

(b) Epiotis, N. D.; Bjorkquist, D.; Bjorkquist, L.; Sarkanen, S. *J. Am. Chem. Soc.* 1973, 95, 7558. (c) Epiotis, N. D.; Sarkanen, S.; Bjorkquist, D.; Bjorkquist, L.; Yates, R. *J. Am. Chem. Soc.* 1974, 96, 4075. (d) Larson, J. R.; Epiotis, N. D.; Bernardi, F. *J. Am. Chem. Soc.* 1978, 100, 5713.

(16) Dimetalated oximes show no significant decomposition after 7 h at room temperature in THF or after 1 h of reflux in THF,<sup>5</sup> whereas metalated oxime ethers decompose at 0 °C.<sup>17</sup>

(17) Spencer, T. A.; Leong, C. W. *Tetrahedron Lett.* 1975, 3889.

metalation onto the  $\alpha$ -carbon cis to the oxime oxygen atom.<sup>6</sup> Recently, one of us suggested that the second metalation on the syn side can be rationalized equally well by the structure proposed by Kofron and Yeh or with an ion cluster structure in which *both* of the metal cations are in bridging positions between the two centers of highest negative charge.<sup>18</sup> A variety of crystal structures of dilithiated compounds has become available in recent years<sup>19</sup> that demonstrate the importance of such a triple ion model. For example, the structures of the TMEDA-solvated dimers of methyl lithiomethyl sulfide<sup>20</sup> and of phenyllithium<sup>21</sup> contain triple ions in which the negative charges are mostly localized in carbon  $sp^3$  or  $sp^2$  orbitals, respectively.

In the present work we report *ab initio* calculations of syn- and anti-configured geometrical isomers of acetaldoxime dianions and dimetalated acetaldoxime. Several possible topological arrangements are discussed for the dimetalated species, and the potential energy surface has been searched for the most reasonable of these structures. Five stationary points have been optimized for dilithioacetaldoxime structures, and four stationary points have been located for the corresponding sodium derivatives (Table I). The regioselectivity in the formation of the metalated enolate equivalents is studied based on the relative energies of the isomeric dianions and of their metalated derivatives. The cation effect on the regioselectivity is examined by comparison of the lithium and sodium derivatives of acetaldoxime. The potential energy surface of dilithioacetaldoxime has also been explored with the semiempirical methods MNDO and AM1, and the results are compared to the *ab initio* data. Mechanistic implications are presented of the theoretical results with respect to the regioselective formation of the syn-configured dimetalated intermediates and to the regioselective entry of electrophiles.

### Computation Aspects

Standard single-determinant restricted Hartree-Fock (RHF) calculations were performed with the program GAUSSIAN82.<sup>22</sup> Stationary structures were optimized simultaneously by using Schlegel's gradient technique<sup>23</sup> under the constraints of the symmetry point group specified. A slightly modified 3-21+G basis set was used for the geometry optimizations: The metal cations were described by the standard 3-21G basis set<sup>24</sup> and the anion in the ion aggregate was described by the 3-21+G basis set<sup>25</sup> resulting from addition of single diffuse  $sp$ -shells to all heavy centers. This choice of basis set, denoted 3-21+G despite the modest modification, provides a more balanced functional description of the associated ions.<sup>26</sup> The structures were used for energy calculations with a modestly modified version of the 6-31+G\* basis set (6-31+G\*/3-21+G).<sup>25,27</sup> No  $d$  functions or diffuse functions

were used for the description of the metal atoms. These functions are not necessary for the proper description of the metal cations but would serve only to increase the number of empty orbitals at the metal atoms and lead to increased basis set superposition error.<sup>26</sup> Harmonic vibrational frequencies<sup>28</sup> were calculated at the level of optimization to characterize stationary points as minima or saddle points<sup>29</sup> and to obtain vibrational zero-point energies. The vibrational zero-point energy corrections to relative energies were scaled (factor 0.9) to account for their general overestimation at this computational level.<sup>30</sup>

Projection electron density functions  $P(x,z)$  of the dianions were calculated at the level of optimization with the program PROJ.<sup>31</sup> Demarcation of spatial regions<sup>32</sup> of  $P(x,z)$  and integrations of the contained projected electron density yield integrated projection populations (IPP). Populations thus obtained are approximations<sup>33</sup> to Bader's populations<sup>34</sup> which are determined by integration within *basins* demarked by the 3-dimensional zero-flux surfaces of the electron density. The approximation of the 3-dimensional zero-flux surfaces by *vertical curtains*<sup>31</sup> is more efficient computationally and provides results sufficient for the present analysis. Moreover, the minimum projected electron density (MPD) at the projection bond critical point BCP<sub>p</sub> of the projection bond path and its location given as the fraction  $F(AB)$ ,  $F = d(A-BCP_p)/d(A-B)$ , yield characteristic information about the electron density distribution.<sup>33</sup>

Semiempirical calculations with the MNDO<sup>35</sup> and AM1<sup>36</sup> Hamiltonians were performed<sup>37</sup> with the lithium parametrization by Clark and Thiel.<sup>38</sup> In our previous studies of the lithium ion pairs of isomeric acetaldoxime carbanions the adequacy of MNDO was evaluated critically<sup>39</sup> by comparison with *ab initio* results.<sup>40,41</sup> Overestimation of the pyramidalization at the carbanionic center and insufficient carbon lone pair-lithium core repulsion were found to cause the following artifacts: excessive charge localization, the breakdown of the pseudo- $\pi$ -conjugation within the ligands, and orbital orientation toward the cation. A simple method was proposed, namely, to constrain the CCH<sub>2</sub> fragment to planarity, to counteract these deficiencies in part, and the results thus obtained are in better agreement with *ab initio* data. This strategum is applied and tested in the present study as well.

(27) (a) Hehre, W. J.; Ditchfield, R.; Pople, J. A. *J. Chem. Phys.* **1972**, *56*, 2257. (b) Hariharan, P. C.; Pople, J. A. *Theoret. Chim. Acta* **1973**, *28*, 213. (c) Binkley, J. S.; Gordon, M. S.; Defrees, D. J.; Pople, J. A. *J. Chem. Phys.* **1982**, *77*, 3654.

(28) Pople, J. A.; Krishnan, R.; Schlegel, H. B.; Binkley, J. S. *Int. J. Quantum. Chem.* **1979**, *S13*, 225.

(29) Murrell, J. N.; Laidler, K. J. *J. Chem. Soc., Faraday Trans.* **1968**, *64*, 371.

(30) Francl, M. M.; Pietro, W. J.; Hehre, W. J.; Gordon, M. S.; Defrees, D. J.; Pople, J. A. *J. Phys. Chem.* **1982**, *77*, 3654.

(31) (a) Streitwieser, A., Jr.; Collins, J. B.; McKelvey, J. M.; Grier, D. L.; Sender, J.; Toczko, A. G. *Proc. Natl. Acad. Sci. U.S.A.* **1979**, *76*, 2499.

(b) Collins, J. B.; Streitwieser, A., Jr.; McKelvey, J. M. *J. Comput. Chem.* **1979**, *3*, 79. (c) Collins, J. B.; Streitwieser, A., Jr. *J. Comput. Chem.* **1980**, *1*, 81.

(32) McDowell, R. S.; Grier, D. L.; Streitwieser, A., Jr. *J. Comput. Chem.* **1985**, *9*, 165.

(33) Glaser, R. *J. Comput. Chem.* **1988**, *9*, 118.

(34) Review: Bader, R. F. W. *Acc. Chem. Res.* **1985**, *18*, 9.

(35) Dewar, M. J. S.; Thiel, W. *J. Am. Chem. Soc.* **1977**, *99*, 4899, 4907.

(36) Dewar, M. J. S.; Zoebisch, E. G.; Healy, E. F. *J. Am. Chem. Soc.* **1985**, *107*, 3902.

(37) Semiempirical calculations were performed with the MOPAC (Version 3.1) program of J. J. P. Stewart (*QCPE Bull.* **1983**, *3*, 43) as implemented into GAUSSIAN86 by M. Frisch.

(38) Thiel, W.; Clark, T. Lithium Parametrization. Unpublished.

(39) Glaser, R.; Streitwieser, A., Jr. *J. Mol. Struct. (Theochem.)* **1988**, *163*, 19.

(40) Glaser, R.; Streitwieser, A., Jr. *J. Am. Chem. Soc.* **1987**, *109*, 1258; *Ibid.*, in press.

(41) Glaser, R.; Streitwieser, A., Jr. *Pure Appl. Chem.* **1988**, *60*, 195.

(18) Streitwieser, A., Jr. *Acc. Chem. Res.* **1984**, *17*, 353.

(19) For a review see: Setzer, W. N.; Schleyer, P. v. R. *Adv. Organomet. Chem.* **1985**, *24*, 353.

(20) Amstutz, R.; Laube, T.; Schweizer, W. B.; Seebach, D.; Dunitz, J. D. *Helv. Chim. Acta* **1984**, *67*, 224.

(21) Thoennes, D.; Weiss, E. *Chem. Ber.* **1978**, *111*, 3157.

(22) Binkley, J. S.; Frisch, M.; Raghavachari, K.; Defrees, D.; Schlegel, H. B.; Whiteside, R.; Fluder, E.; Seeger, R.; Pople, J. A. GAUSSIAN82, Release A Version, Carnegie-Mellon University, 1983.

(23) Schlegel, H. P. *J. Comput. Chem.* **1982**, *3*, 214.

(24) (a) Binkley, J. S.; Pople, J. A.; Hehre, W. J. *J. Am. Chem. Soc.* **1980**, *102*, 939. (b) Gordon, M. S.; Binkley, J. S.; Pople, J. A.; Pietro, W. J.; Hehre, W. J. *J. Am. Chem. Soc.* **1982**, *104*, 2197.

(25) Clark, T.; Chandrasekhar, J.; Spitznagel, G. W.; Schleyer, P. v. R. *J. Comput. Chem.* **1983**, *3*, 294.

(26) (a) Pullman, A.; Berthod, H.; Gresh, N. *Int. J. Quantum Chem.* **1976**, *10*, 59. (b) Hobza, P.; Zahradnik, R. *Chem. Rev.* **1988**, *88*, 871.

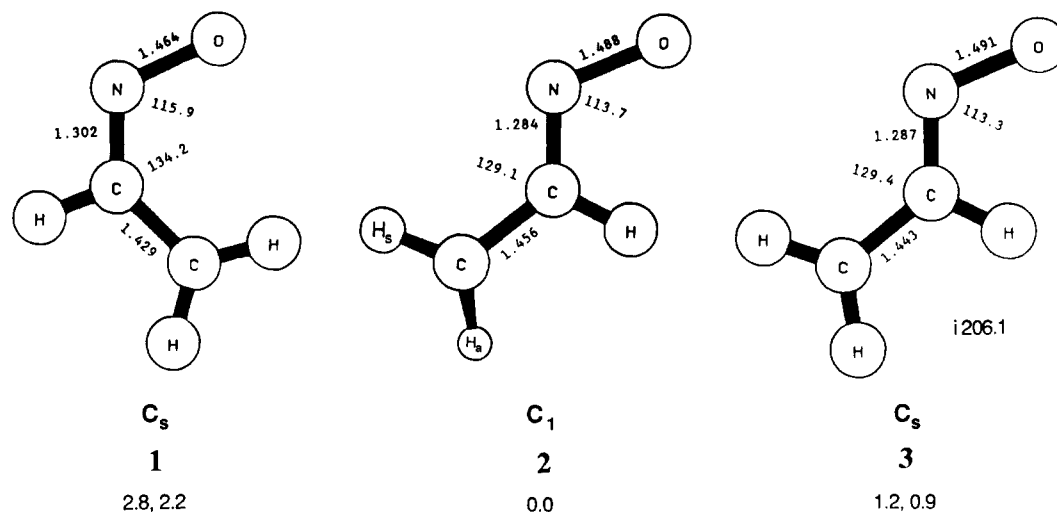


**Figure 1.** Molecular-model-type drawings of isomeric acetaldoxime dianions. The syn-isomer **1** ( $C_s$ ) and the chiral anti-isomer **2** are minima. The planar dianion **3** is the transition state to racemization of **2**. Here and in all other figures relative energies as obtained at the 6-31+G\*//3-21+G level without and with correction by the scaled vibrational zero-point energies calculated at 3-21+G are given in kcal mol<sup>-1</sup>. Transition states are indicated by specification of the imaginary frequency in cm<sup>-1</sup>.

**Table II.** Structures and Integrated Electron Populations of the Isomeric Dianions of Acetaldoxime, **1** ( $C_s$ , syn) and **2** ( $C_1$ , anti), and of the Planar Transition-State **3** to Racemization of **2**

parameter	1	2	3
ON	1.464	1.488	1.491
NC	1.302	1.284	1.287
CC	1.429	1.456	1.443
CH <sub>s</sub>	1.073	1.083	1.079
CH <sub>a</sub>	1.082	1.086	1.080
CH	1.094	1.093	1.093
ONC	115.9	113.7	113.3
NCC	134.2	129.1	129.4
H <sub>s</sub> CC	121.3	118.5	121.8
H <sub>a</sub> CC	119.4	116.7	119.7
HCN	112.0	116.2	116.0
CCNO	0.0	181.8	180.0
H <sub>s</sub> CCN	0.0	-12.8	0.0
H <sub>a</sub> CCN	180.0	202.1	180.0
HCNO	180.0	0.5	0.0
IPP(O) <sup>c</sup>	8.906	8.899 <sup>d</sup>	8.910
IPP(N)	7.714	7.787	7.778
IPP(CH)	6.620	6.527	6.541
IPP(CH <sub>2</sub> )	8.761	8.787	8.770

<sup>a</sup>In angstroms and degrees. <sup>b</sup>The deprotonated carbon atom is italicized. H<sub>s</sub> (H<sub>a</sub>) denotes the hydrogen that is on the same (opposite) side as N. <sup>c</sup>Integrated projected electron population in electrons. <sup>d</sup>Projection for **2** is perpendicular to the ONC plane.

## Results and Discussion

**Isomeric Acetaldoxime Dianions.** Double deprotonation of (*Z*)-acetaldoxime results in the planar syn-configured dianion<sup>42</sup> **1**. For the anti isomer the equilibrium structure, **2**, has been found to be non-planar. In **2** both of the hydrogens of the CH<sub>2</sub> group and the oxygen atom are on the same side of the NCC plane. The angles enclosed between the NCC plane and the HCC planes are 12.8° and 22.1° for the H<sub>s</sub> and the H<sub>a</sub> atoms (see Figure 1), respectively, while the displacement of the oxygen out of the NCC plane is small (the dihedral angle ONCC is 181.8°). The planar structure *anti*-**3** corresponds to a stationary point with one imaginary frequency (i206.1 cm<sup>-1</sup>) and thus represents the transition-state structure for

(42) The eigenvalues of the three highest-lying MOs of 1–3 are positive. These dianions are not stable in the calculated closed-shell configuration in the gas phase. However, such closed-shell dianions do exist in the liquid phase, and our calculations serve to model the dianions in the electronic state it assumes in solution.

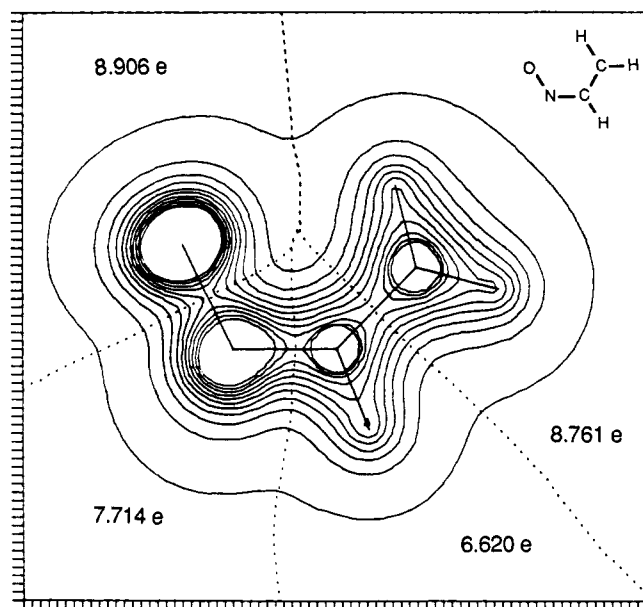


**Figure 2.** Contour plot of the electron density projection function of the syn-configured dianion **1**. Contour levels are from 0.01 to 0.81 e au<sup>-2</sup> with a spacing of 0.08. Demarcation lines are shown as dotted lines.

racemization of the anti enantiomers **2**. The zero-point energy-corrected barrier to racemization is 0.9 kcal mol<sup>-1</sup> at 6-31+G\*//3-21+G. This barrier is sufficiently low that these relative energies could change significantly at higher computational levels.<sup>43</sup> Drawings of the dianions are shown in Figure 1, and structural parameters are listed in Table II.

The formation of the dianions results in small increases of the NO and the CN bond lengths, a decrease of the CC bond length, and an increase by several degrees of the NCC and ONC angles as compared to the neutral acetaldoxime isomers.<sup>40</sup> The changes in bond lengths are consistent with

(43) The barrier at 3-21+G is 0.14 kcal mol<sup>-1</sup> but becomes *negative* when vibrational zero-point corrections are taken into account. At the 3-21+G level one would thus be led to the conclusion that **3** is the minimum and distortion of the  $C_s$  symmetric structure does not occur because of the increase of the vibrational zero-point energy upon distortion. The calculations at 6-31+G\* show that **3** is a transition-state structure: The vibrational zero-point energies of **2** and **3** reduce the barrier, but **3** remains higher in energy.

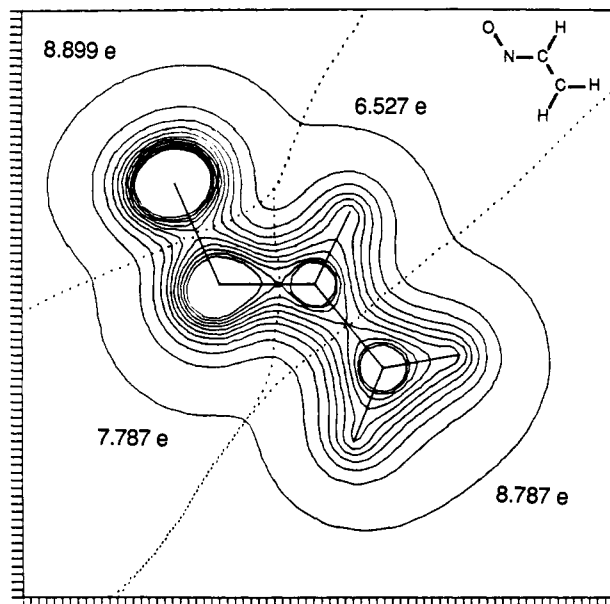


Figure 3. Contour plot of the electron density projection function of the anti-configured dianion 2. The projection was carried out perpendicular to the ONC plane. See Figure 2 for details.

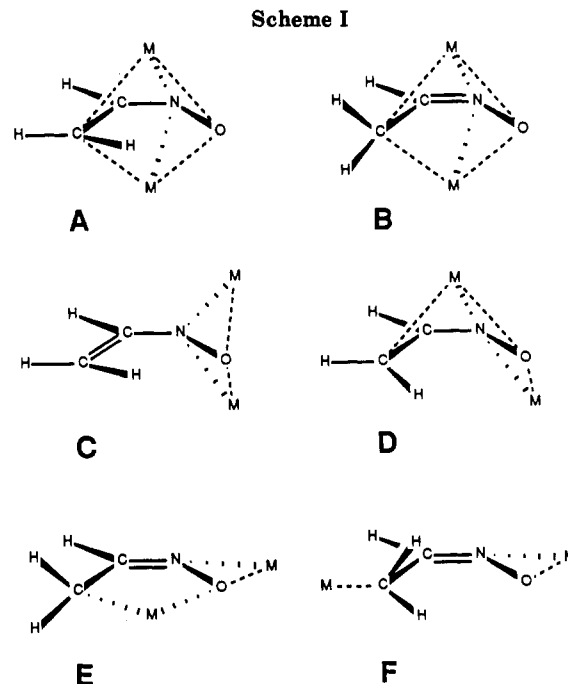
Table III. Selected Bond Lengths and Angles of the Dianions in the Isomeric Dimetalated Acetaldoximes<sup>a</sup>

molecule	ON	NC	CC	ONC	NCC
4	1.542	1.371	1.357	110.3	128.6
5	1.549	1.397	1.339	110.2	129.8
6	1.484	1.275	1.508	118.1	127.0
7	1.473	1.286	1.533	114.0	124.6
8	1.562	1.400	1.336	108.6	125.6
9	1.421	1.311	1.421	114.7	120.4
10	1.516	1.355	1.366	109.5	129.7
11	1.521	1.344	1.369	112.3	129.1
12	1.543	1.363	1.351	110.1	127.2
13	1.547	1.359	1.358	108.8	125.8

<sup>a</sup>In angstroms and degrees.

the nodal properties of the highest occupied  $\pi$ -MO, 3a''. The 3a'' MO has one node in the CC bonding region in the neutral oxime and in the monoanion. The second deprotonation at carbon causes this node to be shifted into the CN bonding region; hence, the CC bond decreases and the CN bond increases.

The anti-dianion 2 has been found to be thermodynamically favored over the syn isomer by 2.2 kcal mol<sup>-1</sup> at the highest level (Table I). The thermodynamic preference for the anti dianion is attributed primarily to electrostatic repulsion effects. Electron density analysis of the dianions 1 and 2 (Figures 2 and 3) shows that the charge on the CH<sub>2</sub> group is -0.8 for all of the dianions and that the heteroatoms carry the major fractions of the negative charge (Table III). The syn isomer becomes destabilized by the repulsive interaction between the carbanionic center and both of the highly charged heteroatoms, whereas the anti isomer is destabilized primarily by the repulsive interaction only between the carbanionic center and nitrogen. The strong electrostatic repulsion in the syn-isomer 1 manifests itself in the geometry and in the electronic structure. The NCC and ONC bond angles in 1 are 134.2° and 115.9°, respectively, and are both larger in the syn isomer compared to the anti isomer ( $\Delta$ (NCC) = 5.2° and  $\Delta$ (ONC) = 2.2°). The IPP values indicate nearly equal charges on the CH<sub>2</sub> groups in all of the dianions, but pyramidalization of the CH<sub>2</sub> group of the anti-isomer 2 puts more charge on one side and serves to orient the electron density at that carbon away from the heteroatoms.



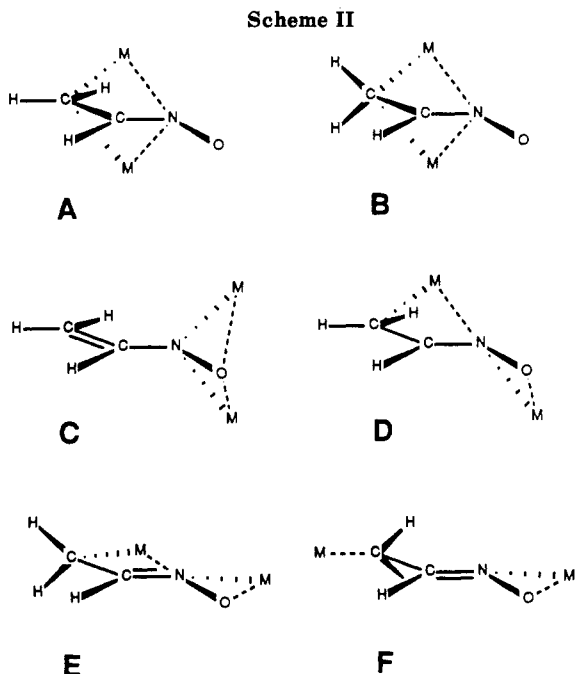
The relative energies of the isomeric dianions show that the regioselective formation of the syn-configured dimetalated derivative of oximes is not a property of the dianion itself as had been suggested by Jung et al.<sup>5</sup> and Lyle et al.<sup>7</sup> These workers considered the syn dianion to be thermodynamically favored due to nonbonded through-space homoconjugation. Such homoconjugation requires bonding  $\pi$ -overlap between the carbanionic center and the oxygen atom. Cross sections of the electron density in planes that are parallel to the molecular plane would exhibit electron density accumulation between these atoms and a (3,+1) ring critical point<sup>34</sup> would occur in a central position of the homoconjugated system and a (3,-1) bond critical point would exist along the bond path connecting the two atoms. Projection of the 3-dimensional electron density distribution into the molecular plane would lead to the corresponding projection critical points<sup>33</sup> (2,+2)<sub>p</sub> and (2,0)<sub>p</sub> of the electron density projection function. Such projection critical points are not present in the electron density projection function of 1 (Figure 2). Homoconjugation is thus unimportant in the syn dianion of acetaldoxime 2.

**Topological Arrangements for Dimetalated Acetaldoxime.** The association of each of the isomeric acetaldoxime dianions with cations can lead to a variety of topologically different modes of coordination<sup>44</sup> as shown in Schemes I and II for the syn- and the anti-configured isomers, respectively.

In the triple ion structures *syn*-A and *syn*-B both cations are in  $\eta^4$ -face coordinating positions and could bridge between the carbanionic center and the oxygen in either a symmetrical ( $C_s$ ) or asymmetrical ( $C_1$ ) fashion. The structures of type *syn*-A and *syn*-B differ with regard to the hybridization at the carbanionic carbon.<sup>45</sup> If the  $\pi$ -system within the dianion remains intact in the triple ion, then the carbanionic center assumes an sp<sup>2</sup> hybrid-

(44) For reviews on dimetalated structures, see: (a) Schleyer, P. v. R. *Pure Appl. Chem.* 1983, 55, 355. (b) Schleyer, P. v. R. *Pure Appl. Chem.* 1984, 56, 151. (c) Maercker, A.; Thies, M. *Top. Curr. Chem.* 1987, 138, 1.

(45) Schleyer, P. v. R.; Kos, A. J.; Wilhelm, D.; Clark, T.; Boche, G.; Decher, G.; Etzrodt, H.; Dietrich, H.; Mahdi, W. *J. Chem. Soc., Chem. Commun.* 1984, 1495.



ization, as in *syn-A*, and the electrostatic interaction between the cations and the dianion involves  $\pi$ -charge density at the  $\text{CH}_2$  carbon. Breakdown of the conjugation within the dianion, assumption of an  $\text{sp}^3$  hybridization at the  $\text{CH}_2$  carbon, and rotation of the  $\text{CH}_2$  group in order to orient the carbon lone pair between the metal cations would result in a structure of the type *syn-B*. A triple ion structure of type *syn-B* could be electrostatically favored over the type *syn-A* because the centers of the triple ion are closer together;<sup>46</sup> however, the loss of conjugative stabilization may still be too great. A third possible triple ion structure, *syn-C*, results from  $\eta^2$ -NO bond coordination by both of the cations. The anti versions of the triple ion structures A and B are clearly unimportant as the oxygen would be left uncoordinated, whereas *syn-C* finds a reasonable counterpart in the doubly  $\eta^2$ -NO-bridged structure of the type *anti-C*.

In the structure types *syn-D* and *anti-D* one of the cations is formally  $\eta^4$ - or  $\eta^3$ -face coordinating, respectively, while the other cation either coordinates solely to the oxygen or bridges the NO bond. Pyramidalization at the carbanionic center converts these structures into structures of type E. The structure of dimetalated oximes suggested by Kofron and Yeh<sup>6</sup> corresponds to the *syn-E* type: one cation engages in a 1,4-(C,O)- $\sigma$ -bridge while the other is coordinated only by oxygen or by both of the heteroatoms.

Structures of type F in which each of the cations is associated only with one of the centers of charge should clearly be disfavored, and such structures need therefore not be considered.

**Dilithioacetaldoxime.** Selected bond lengths and bond angles of the dianions in the metalated derivatives and major bond lengths involving the cations are summarized in Tables III and IV, respectively. Complete structures are given in appendix I (supplemental material; see the paragraph at the end of the paper).

A structure of the *syn-D* type is found as the global minimum on the potential energy surface of dilithioacetaldoxime, and molecular-model-type drawings of this chiral structure 4 are shown in Figure 4. In 4 one of the lithium cations, Li1, engages in a formal  $\eta^4$ -face coordi-

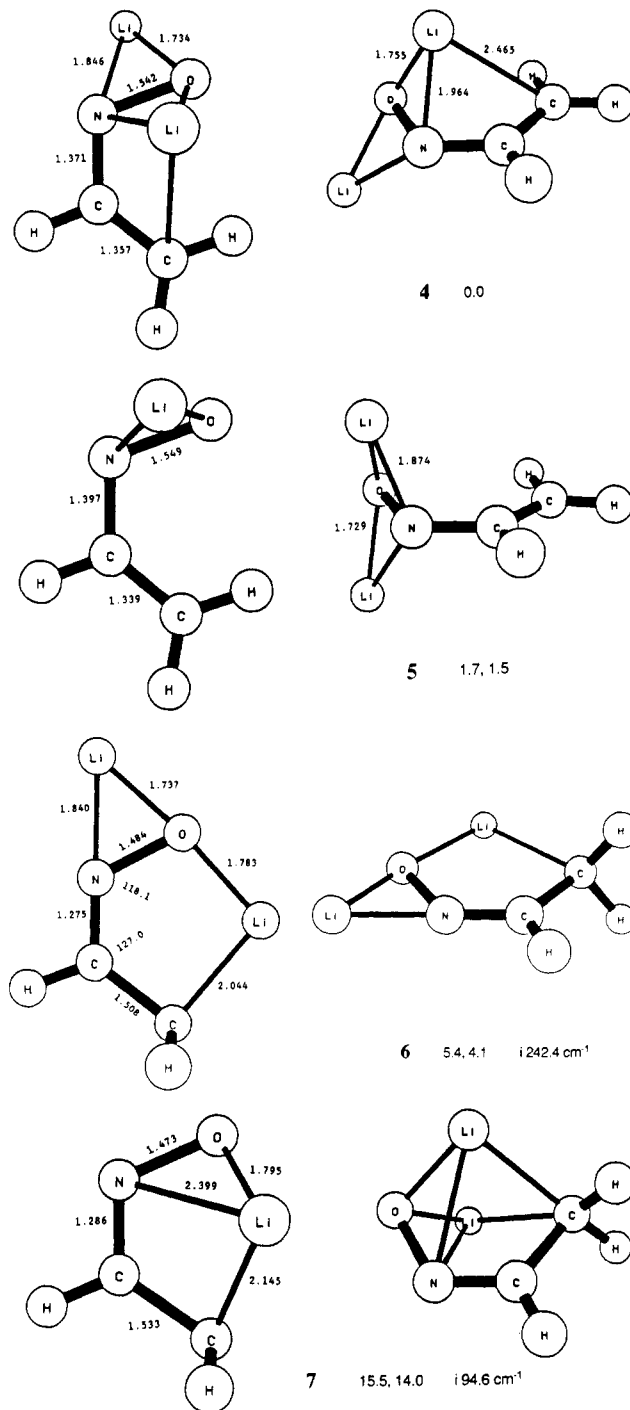


**Figure 4.** Molecular-model-type drawings of various stationary structures of dilithio-(*Z*)-acetaldoxime: the global minimum 4 ( $C_1$ ), the puckered triple ion 5 ( $C_2$ ), and two transition structures, 6 ( $C_3$ ), the transition state for racemization of 4, and 7 ( $C_3$ ), a triple ion structure with the negative poles centered at O and the carbanionic carbon. Relative energies are given as specified in Figure 1.

nation while the other lithium, Li2, bridges the NO bond in a  $\eta^2$ -fashion. This structure is a combination of the  $\eta^4$ - and  $\eta^2$ -coordinated structures found previously as structures of the lithium ion pair of acetaldoxime carbanion.<sup>40,41</sup> In both cases short contacts between the cation and the heteroatoms and long bond distances between the  $\text{CH}_2$  carbon and  $\text{Li}^+$  were found. Both of the lithium-heteroatom distances are slightly shortened compared to the  $\eta^4$ -coordinated lithium ion pair of acetaldoxime carbanion. The bond distances between the  $\eta^2$ -coordinating Li2 and

(46) Streitwieser, A., Jr. *J. Organomet. Chem.* 1978, 156, 1.

Table IV. Major Bond Lengths (angstroms) Involving the Cations

molecule	MC(C)	MC(N)	MN	MO	MM
4	2.465	2.265	1.964	1.755	3.227
	3.847	3.003	1.846	1.734	
5	3.389	2.745	1.874	1.729	3.115
	2.044	2.601	2.590	1.783	3.515
6	4.200	3.115	1.840	1.737	
	2.145	2.449	2.399	1.795	2.440
7	2.145	2.449	2.399	1.795	2.440
	3.812	2.785	1.861	1.734	3.021
8	2.134	2.165	1.873	3.122	4.647
	5.197	3.822	2.998	1.597	
9	3.050	2.602	2.135	2.018	3.839
	2.631	2.461	2.193	2.026	3.636
10	4.232	3.255	2.025	2.038	
	3.898	2.928	2.051	2.044	3.531
11	3.146	2.482	2.093	2.067	3.506
	4.321	3.240	2.012	2.054	

O and N are 1.734 and 1.846 Å, respectively; the LiO distance is thus somewhat shorter compared to the  $\eta^2$ -NO bond coordinated isomer of the lithium acetaldoxime carbanion,<sup>40</sup> while the LiN distance is slightly elongated. Both of the contacts between Li2 and the heteroatoms are shorter compared to Li1 and, in particular, Li2N is 0.118 Å shorter than Li1N. The four-membered ring thus formed by the lithiums and the heteroatoms is slightly puckered and places the cations 3.227 Å apart.

In the attempt to locate a stationary structure of type *syn-A*, the  $C_s$  symmetric structure<sup>47</sup> 5 of type *syn-C* was obtained (Figure 4). The vibrational frequencies showed this structure to be a local minimum. Obviously, charge localization on the heteroatoms ("1,2-dianion") and triple ion formation in this way is energetically favorable over charge delocalization ("1,4-dianion") and triple ion formation of the type *syn-A*. Structure 5 is only 1.7 kcal mol<sup>-1</sup> higher in energy than 4 at 6-31+G\*\*//3-21+G, and the inclusion of vibrational zero-point energy corrections reduces the energy difference to 1.5 kcal mol<sup>-1</sup>. This structure can be compared to the  $\eta^2$ -NO bond coordinated lithium ion pair of acetaldoxime carbanion.<sup>40</sup> The second metalation causes the lithium-oxygen contact to become stronger ( $\Delta(\text{LiO}) = -0.060$  Å), whereas the lithium-nitrogen distance is increased ( $\Delta(\text{LiN}) = 0.056$  Å) to about the same extent. The triple ion formed between the lithiums and the heteroatoms (LiLi = 3.115 Å) is puckered in a way that places the cations away from the carbon atoms. The CC and CN bonds are 1.339 and 1.397 Å, respectively, in 5 and indicate that 5 is best described as the dilithio derivative of vinylhydroxylamine. Note that the CC and CN bond lengths in 5 are much closer to the corresponding bond lengths in 1 than in 4. This finding suggests that the formation of 4 is accompanied by strong internal charge transfer toward the heteroatoms and that 4 might be better described as a triple ion with the heteroatoms as the negative centers.

A  $C_s$  symmetric structure of type *syn-E*, shown in Figure 4, has been suggested by Kofron and Yeh<sup>6</sup> as the intermediate formed by metalation of (*Z*)-acetaldoxime. One of the lithium atoms, Li1, engages in a 1,4-(C,O)- $\sigma$ -bridge and Li2 bridges between the heteroatoms. However, this structure does not correspond to a local minimum; one of the vibrational frequencies is imaginary ( $i242.4$  cm<sup>-1</sup>), and its normal mode<sup>48</sup> identifies 6 as the transition structure

(47) Professor P. v. R. Schleyer and Dr. A. J. Kos have obtained a similar structure at 3-21G. Private communication.

(48) The transition vector  $[x,y,z]$  of 6 (N at the origin, the NC bond defines the  $z$  axis, and the molecule lies in the  $xz$  plane): N 0,0,0; C (N) 0,-0.08,0; C (C) 0,0,0; O 0,0.08,0; H (CH<sub>2</sub>) 0.28,0.39,-0.47; H (CH<sub>2</sub>) -0.28,0.39,0.47; H (CH) 0,-0.26,0; Li (OC bridging) 0,-0.13,0; Li (NO bridging) 0,0.01,0.

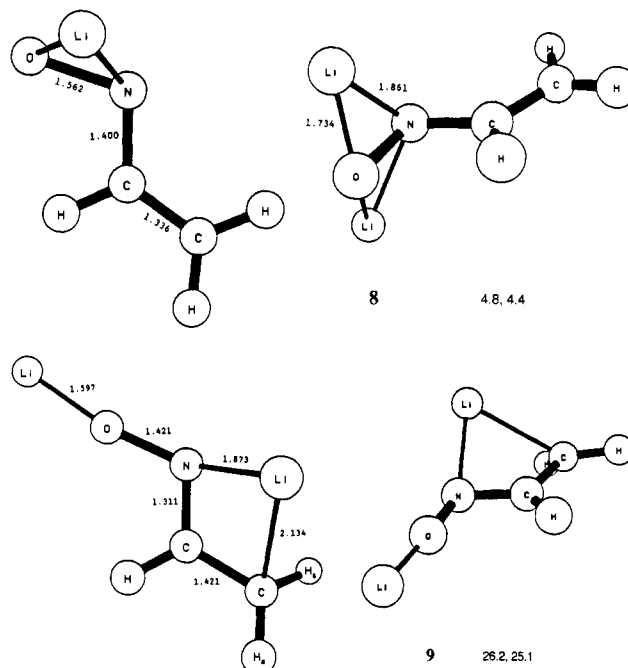


Figure 5. Molecular-model-type drawings of the anti- or *E*-configured dilithio derivative of acetaldoxime: the most stable structure, 8 ( $C_s$ ), having 2-fold  $\eta^2$ -NO bond coordination, and the less stable structure 9 ( $C_1$ ).

for racemization of the global minimum 4. The activation barrier to racemization is 5.4 kcal mol<sup>-1</sup> at 6-31+G\*\*//3-21+G; inclusion of the vibrational zero-point energy correction results in the value of 4.1 kcal mol<sup>-1</sup>.

A structure of the type *syn-B*, 7 (Figure 4), corresponds to a stationary point on the energy surface. Localization of charge at the carbanionic center results in short LiC bonds of 2.145 Å in 7. The LiN contact is unimportant in this symmetrically 1,4-(C,O)- $\sigma$ -bridged triple ion. The normal modes indicate one imaginary frequency ( $i94.6$  cm<sup>-1</sup>) and characterize 7 as a transition state, apparently for CH<sub>2</sub> rotation.<sup>49</sup> Structure 7 is 15.5 kcal mol<sup>-1</sup> less stable than 4 at 6-31+G\*\*//3-21+G and the inclusion of the zero-point energy corrections reduces this barrier to 14.0 kcal mol<sup>-1</sup>.

The most stable structure for the dilithiated anti-configured dianion is  $C_s$  symmetric and of type *anti-C*. This doubly  $\eta^2$ -NO bond coordinated structure 8, best described as an isomer of the dilithio derivative of vinylhydroxylamine 5, is shown in Figure 5. This structure is related to the  $\eta^2$ -NO bond coordinated lithium ion pair of acetaldoxime anti carbanion.<sup>40</sup> Introduction of the second lithium leads to enhancement of the lithium-oxygen contact but an increase in the LiN distance, as also found for the corresponding *syn*-isomer 5. The triple ion consisting of the lithiums and the heteroatoms (LiLi = 3.021 Å) is puckered as in 5. The CC and CN bonds (1.336 and 1.400 Å, respectively) are virtually identical for 8 and its *syn*-isomer 5. 8 is 3.2 kcal mol<sup>-1</sup> less stable compared to 5 at 6-31+G\*\*//3-21+G and inclusion of vibrational zero-point energies gives a value of 2.9 kcal mol<sup>-1</sup>. The *syn* preference of this pair of isomeric compounds is attributed to the additional stabilization arising from cation-induced polarization of the  $\pi$ -electron density in 5. This polarization

(49) The transition vector  $[x,y,z]$  of 7 (N at the origin, the NC bond defines the  $z$  axis, and the molecule lies in the  $xz$  plane): N 0,0.12,0; C (N) 0,0.14,0; C (C) 0,-0.11,0; O 0,-0.17,0; H1 (CH<sub>2</sub>) -0.07,-0.40,0.35; H2 (CH<sub>2</sub>) 0.07,-0.40,-0.35; H (CH) 0,0.43,0; Li1 -0.27,0.06,-0.04; Li2 0.27,0.06,0.04.

causes the angle between the two LiNO planes (syn 148.3°, anti 138.8°) to be larger in **5** than in **8**.

A structure of type *anti*-D, **9** (Figure 5), is found as a second minimum for the anti-configured dilithio acetaldoxime; **9** is 20.7 kcal mol<sup>-1</sup> less stable than **8** at the highest level. In **9** one of the lithium cations, Li1, is  $\eta^3$ -face coordinating, and the other lithium, Li2, is placed at the oxygen almost along the NO axis (deviation 9°) and with a short LiO bond length of 1.597 Å. Attempts to find a local minimum in which Li1 remains  $\eta^3$ -coordinating and Li1 engages in a bridging position between the heteroatoms were unsuccessful; structures **8** or **9** were obtained in all of these attempts. The H<sub>s</sub>-(H<sub>a</sub>) atom is moved out of the NCC plane by 45.8° (9.7°) and away (toward) Li1. This modest pyramidalization at the carbanionic center results in a shorter Li1C contact and a reduced dihedral angle compared to the  $\eta^3$ -coordinated lithium ion pair of acetaldoxime anti carbanion.<sup>40,39</sup> In **4** such pyramidalization is practically unimportant as the cation tends to enhance its chelation by oxygen.

The calculations of the dimetalated derivatives show a preference for the syn isomer in agreement with experiment. Whereas the anti-configured dianion is favored compared to the syn isomer, for the dilithium triple ion the syn configuration **4** is the global minimum and it is preferred over the most stable anti-configured isomer **8**. Our theoretical results are thus in agreement with the experimentally observed regioselectivity, and such dimetalated oximes should be considered in reaction mechanisms (*vide infra*). The syn preference energy is 4.8 kcal mol<sup>-1</sup> at 6-31+G\*\*/3-21+G, and the inclusion of vibrational zero-point energies results in a relative energy of 4.4 kcal mol<sup>-1</sup>.

**Cation Effect on Structures and Relative Energies. Sodium versus Lithium.** Two minimum-energy structures have been located for sodium derivatives of (*Z*)-acetaldoxime, **10** and **11** (Figure 6), that correspond topologically to the dilithioacetaldoximes **5** and **4**, respectively. **10** is a C<sub>s</sub> symmetry doubly  $\eta^2$ -NO-bond bridged structure, and **11** is a chiral structure<sup>50</sup> in which one of the sodium cations, Na1, is formally face-coordinating while the other cation, Na2, is placed in a  $\eta^2$ -NO-bond bridging position.

Replacement of Li<sup>+</sup> by Na<sup>+</sup> enhances the interaction between the cation and the heteroatoms (Table IV). This tendency was found previously for the ion pairs formed by acetaldoxime carbanions.<sup>40,41</sup> The increases of the bond lengths between Na<sup>+</sup> and nitrogen and, in some cases, oxygen compared to Li<sup>+</sup> are smaller than the difference of the ionic radii<sup>51</sup> of the cations. The metal-heteroatom distances in **10** are increased by  $\Delta(\text{MN}) = 0.261$  Å and  $\Delta(\text{MO}) = 0.289$  Å compared to **5**, and the corresponding changes in bond lengths in **11** compared to **4** are  $\Delta(\text{MN}) = 0.229$  Å and  $\Delta(\text{MO}) = 0.271$  Å for the Na1 and  $\Delta(\text{MN}) = 0.179$  Å and  $\Delta(\text{MO}) = 0.304$  Å for Na2, respectively. In all cases the increase is larger for the MO bonds compared to the MN bonds. The distance between the formally face-coordinating sodium and the carbanionic center remains long in the sodium derivative **11**; the increase of the MC distance is  $\Delta(\text{MC}) = 0.176$  Å compared to the lithium derivative.

(50) Based on the analytically calculated Hessian matrix, this structure does not satisfy the default thresholds for optimization. However, the deviations of the RMS force (0.0004) and of the RMS displacements (0.0026) from the default thresholds (RMS force 0.0003; RMS displacement 0.0012) are small, and **11** was thus not further optimized.

(51) The difference in the ionic radii of Li<sup>+</sup> and Na<sup>+</sup> varies over the range 0.20–0.35 Å on different scales: Cotton, F. A.; Wilkinson, G. *Advanced Inorganic Chemistry*, 4th ed.; Wiley: New York, 1980; p 14.

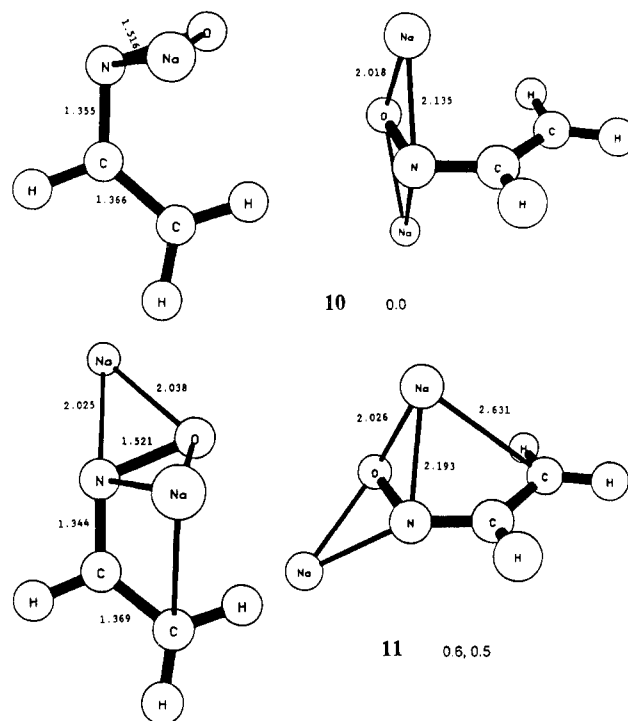


**Figure 6.** Molecular-model-type drawings of the sodium derivative of (*Z*)-acetaldoxime dianion: the most stable structure, **10** (C<sub>s</sub>), with 2-fold  $\eta^2$ -NO bond coordination resulting in a triple ion centered at the heteroatoms, and **11** (C<sub>1</sub>), in which one of the sodium cations engages formally in a  $\eta^3$ -face coordination and the other Na<sup>+</sup> bridges the NO bond.

The doubly  $\eta^2$ -NO-bond bridged structures **10** and **5** exhibit an interesting cation effect. It has been noted above that the triple ion in the lithium derivative is puckered in a way that leaves the cations and the carbanionic center on different sides of the plane that is perpendicular to the NCC plane and that contains the heteroatoms. This equilibrium structure appears to result from the balance between optimization of the electrostatic interaction between the lithiums and the N<sub>s</sub> lone-pair density and the concomitant increase in LiLi repulsion. In the case of sodium, however, the triple ion is puckered in the *opposite* direction; the angle between the NaON and the NCC planes is 84.7°. Optimization of the electrostatic interaction between the sodium cations and the N<sub>s</sub> lone-pair electron density without significant increase of the sodium-heteroatom distances would probably place the sodiums too close to each other.

The two structures **10** and **11** are close in energy. At the 6-31+G\*\*/3-21+G level the symmetric triple ion **10** is favored over the chiral structure **11** by only 0.6 kcal mol<sup>-1</sup> (0.5 kcal mol<sup>-1</sup> with vibrational zero-point energy corrections). The interconversion of the two structures into each other should be a very facile process since the appropriate normal modes have low frequencies.

The C<sub>s</sub> symmetric triple ion **12** of type *anti*-C is shown in Figure 7. **12** is analogous to the lithium derivative **8** and provides an instructive example on how the cation may influence the structure of the ligand. As in the case of the sodium derivatives of the syn-configured dianion, it is found that sodium prefers stronger interactions with nitrogen than with oxygen. The increases of the MN and the MO bonds compared to **8** are  $\Delta(\text{MN}) = 0.190$  Å and  $\Delta(\text{MO}) = 0.310$  Å, respectively. Replacement of Li<sup>+</sup> by Na<sup>+</sup> causes the CC bond to increase by 0.015 Å while the CN bond length decreases by 0.037 Å. Although small, these structural changes indicate that the coordination of



**Table V. Major Structural Parameters and Heats of Formation of the Dianion in Syn- (M1-M4) and Anti- (M5-M8) Configured Isomers of Dilithiated Acetaldoxime As Derived by MNDO and AM1<sup>a-c</sup>**

molecule	method	ON	NC	CC	ONC	NCC	$\Delta H_f$	$\Delta H_f$
M1, C <sub>s</sub>	MNDO	1.276	1.345	1.551	116.8	126.0	-30.68	
	AM1	1.265	1.329	1.516	120.2	127.7		24.15
M2, C <sub>s</sub>	MNDO	1.307	1.322	1.508	119.6	127.8	-27.64	
	AM1	1.296	1.312	1.481	122.1	129.4		29.15
M3, C <sub>s</sub>	MNDO	1.289	1.367	1.497	113.9	126.3	-15.15	
	AM1	1.267	1.351	1.485	117.1	125.9		34.52
M4, C <sub>1</sub>	MNDO	1.325	1.353	1.425	117.9	130.9	-12.95	
	AM1	1.318	1.336	1.414	119.4	130.5		39.70
M5, C <sub>s</sub>	MNDO	1.267	1.332	1.517	119.7	117.3	-17.06	
	AM1	1.257	1.327	1.486	120.9	121.4		35.43
M6, C <sub>1</sub>	MNDO	1.279	1.369	1.437	118.2	119.5	-2.53	
	AM1	1.302	1.361	1.419	117.3	123.0		47.37
M7, C <sub>s</sub>	MNDO	1.212	1.389	1.557	121.8	116.2	-17.00	
	AM1	1.213	1.363	1.521	122.4	118.8		24.10
M8, C <sub>s</sub>	MNDO	1.204	1.399	1.564	120.2	119.0	-3.62	
	AM1	1.207	1.374	1.525	120.7	121.9		33.82

<sup>a</sup> Bond lengths in angstroms, angles in degrees, and  $-\Delta H_f$  in kcal mol<sup>-1</sup>. <sup>b</sup> The CCH<sub>2</sub> fragment was constrained to planarity during optimization of M4 and M6. <sup>c</sup> Structures M3 and M8 can be obtained only by constraining the CCH<sub>2</sub> group to planarity.

N by Na<sup>+</sup> causes an electronic reorganization within the dianion that increases the effective electron density at N compared to Li<sup>+</sup> and thus synergetically reinforces the preference of sodium to coordinate with nitrogen.

The vibrational frequencies identify **12** as a transition-state structure, whereas the lithium analogue is a minimum. The displacement vector<sup>52</sup> of the imaginary normal mode (179.1 cm<sup>-1</sup>) indicates **12** to be metastable with respect to displacements of the sodium cations parallel to the NO bond but in opposite directions. Reoptimization of **12** without symmetry constraints resulted in the chiral structure **13** (Figure 7). The distance of the cation that is trans to the carbon atoms with respect to the NO bond, Na1, is 2.012 and 2.054 Å, respectively, away from N and O, and the Na1ON and ONC planes enclose an angle of 52.7°. Both of the contacts between the other cation, Na2, and the heteroatoms are longer (NaO = 2.067 Å and NaN = 2.093 Å). The skeleton of the acetaldoxime is significantly distorted from planarity; the angle between the planes ONC and NCC is 27.0° and the CH<sub>2</sub> group is moved with respect to the ONC plane toward Na2. Structure **13** is more stable than **12** by 1.7 kcal mol<sup>-1</sup> at the level of optimization, and the inclusion of vibrational zero-point energy corrections does not change this relative energy. However, at 6-31+G\*/3-21+G the energetic ordering is reversed; at this level **13** is less stable by 1.3 kcal mol<sup>-1</sup>. Structure **13** thus appears to be an artifact. The cause for the preference of the chiral structure **13** at the 3-21+G level is not clear but insufficient flexibility of the 3-21+G basis set to account for polarization is a likely cause. The stabilization energy associated with cation-induced polarization of the electron density of the C<sub>2</sub>H<sub>3</sub> fragment is sensitive to distance; this energy term depends on the negative fourth power of the distance between the cation and the center of the induced dipole.<sup>53</sup> In the symmetric structure **12** the distances between the CH and the CH<sub>2</sub> carbons and the sodium cations are 2.928 and 3.898 Å, respectively. The corresponding distances involving Na2 in **13** are 2.482 and 3.486 Å, respectively. The closer approach of Na2 to the C<sub>2</sub>H<sub>3</sub> fragment in **13** increases the charge/induced-dipole interaction compared to **12**. At the higher basis set level, 6-31+G\*, the optimization of the cation/induced-dipole

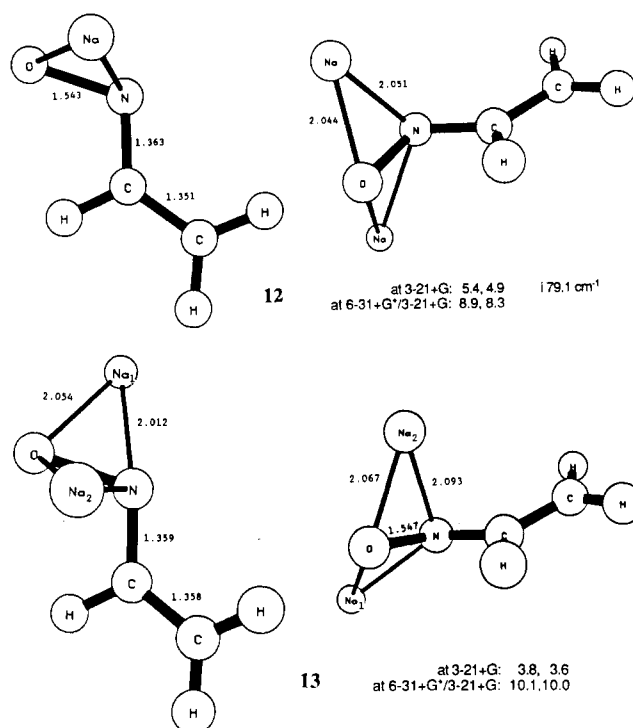


**Figure 7.** Molecular-model-type drawings of disodium derivatives of the anti- or Z-configured acetaldoxime dianion: the more stable symmetric structure **12** (C<sub>s</sub>) and the unsymmetric **13** (C<sub>1</sub>).

interaction does not necessarily require distortion of the C<sub>s</sub> symmetric structure. Instead, the polarization functions may allow for sufficient polarization of the electron density of the C<sub>2</sub>H<sub>3</sub> fragment toward the cations while the symmetric triple ion arrangement between the cations and the heteroatoms persists.

A stationary point corresponding to a structure of type anti-D, analogous to the lithium derivative **9**, does not exist on the 3-21+G potential energy surface. Attempts to obtain a structure of this topology resulted in the chiral structure **13**.

The syn preference of the sodium derivatives is 8.9 kcal mol<sup>-1</sup> at 6-31+G\*/3-21+G, and the inclusion of vibrational zero-point corrections gives 8.3 kcal mol<sup>-1</sup>. The syn preference energy is thus significantly larger for Na<sup>+</sup> compared to Li<sup>+</sup>. This result suggests that larger regioselectivity may be achieved by use of organometallic bases with larger cations in metalations of oximes. Furthermore,

(52) The transition vector  $[x,y,z]$  of **12** (N at the origin, the NC bond defines the z axis, and the molecule lies in the xz plane): N 0,0,23,0; C (N) 0,-0,04,0; C (C) 0,-0,44,0; O 0,0,05,0; H1 (CH<sub>2</sub>) 0,-0,58,0; H2 (CH<sub>2</sub>) 0,-0,52,0; H (CH) 0,0,06,0; Na1 -0,21,0,01,-0,10; Na2 -0,12,0,06,-0,22.

(53) For a related discussion see: Streitwieser, A.; Rajca, A.; McDowell, R. S.; Glaser, R. *J. Am. Chem. Soc.* 1987, 109, 4184.

the syn-preference energies of the dimetalated oximes are larger than the syn-preference energies found for metalated oxime ethers for both of the cations.<sup>40,41</sup>

#### Comparison of MNDO, AM1, and ab Initio Results.

A structure of type *syn-B*, M1 ( $C_s$ ), corresponds to the global minimum on the MNDO potential energy surface of dilithioacetaldoxime (Table V). A structure of type *syn-E*, M2 ( $C_s$ ), is only 3.1 kcal mol<sup>-1</sup> less stable than M1. Both of these structures are transition-state structures at the ab initio level! The structure M3, type *syn-A*, can be obtained only under the constraint of  $C_s$  symmetry, and M1 is obtained otherwise. However, a structure of the type M3 does not correspond to a stationary point on the ab initio surface; attempts to find such a structure resulted in the doubly NO-bridged structure 5. A structure that topologically resembles the global minimum 4 on the ab initio surface, M4, can be obtained only when the CCH<sub>2</sub> group is kept planar during optimization. Complete optimization results in pyramidalization of the carbanionic carbon, artificial charge localization, and orientation of the carbon lone pair toward the cation and leads to M2. The constraint of the CCH<sub>2</sub> fragment to planarity thus proves successful to prevent the breakdown of the pseudo- $\pi$ -conjugation within the dianion.<sup>39</sup> Nonetheless, the structural parameters of M4 deviate significantly from the ab initio structure 4: The formally face-coordinating Li<sup>+</sup> is too close to the carbanionic carbon (2.083 Å) and the LiN contact appears to be unimportant. The characteristic triple ion formed by the cations and the heteroatoms in 4 is not reproduced in M4.

The structures obtained for the dilithio derivatives of the anti-configured dianion of acetaldoxime exhibit similar artifacts. The most stable minimum on the MNDO potential energy surface for such structures is M5 ( $C_s$ ), a structure in which Li1 is 1.3-(C,N)- $\sigma$ -bridging and Li2 coordinates to oxygen only. However, the ab initio calculations have shown that the pseudo- $\pi$ -conjugation is maintained (compare 8). Constraining the CCH<sub>2</sub> fragment to planarity during optimization prevents the breakdown of the  $\pi$ -conjugation and results in a structure, M6, that is in significantly better agreement with the ab initio result. Methodological deficiencies remain apparent for M6 despite this improvement. The LiC contact remains too strong (2.056 Å) and the heat of formation places M6 14.5 kcal mol<sup>-1</sup> above M5. Structures M7 (type *anti-B*) and M8 (type *anti-A*) provide further examples for the inherent deficiencies of the LiC parametrization. Severe overestimation of the LiC contacts causes the entirely unreasonable structure M7 to become a minimum on the MNDO surface that is only 0.1 kcal mol<sup>-1</sup> above M5 despite the fact that oxygen is left uncoordinated!

The AM1 potential energy surface of lithioacetaldoxime was also searched for the stationary structures corresponding to M1–M8. In general, the use of the AM1 Hamiltonian results in more compact structures of the dianions in the triple ions (Table V), and the strengths of the metal contacts are reduced. With the exception of the structures M5 and M6, the topological characteristics are common to the MNDO and AM1 potential energy surfaces. In the MNDO structures M5 and M6 the Li<sup>+</sup> that coordinates solely to oxygen, Li2, is located close to the NO axis (Li–O–N > 170°). In the AM1 structure corresponding to M5 this lithium is moved toward the CH group, and a significantly bent Li–O–N fragment results. The AM1 optimization of M6 moves Li2 into an  $\eta^2$ -NO-bridging position in which the plane defined by lithium and the heteroatoms is almost perpendicular to the best plane of the dianion skeleton, and a structure of the type

*anti-D* results. The relative stabilities of the syn-configured triple ions determined by AM1 are qualitatively similar compared to the MNDO results (Table V). The semiempirical estimate of the relative stabilities of the anti-configured triple ions is not improved by use of the AM1 Hamiltonian. In contrast, on the AM1 potential energy surface M7 is 11.3 kcal mol<sup>-1</sup> more stable than M5, and even the structure M8 is still 1.6 kcal mol<sup>-1</sup> more stable than M5. The structure M6, the structure that most closely resembles the most stable ab initio minimum of the anti-configured triple ion, is the least stable structure among M5–M8 at the AM1 level, and it can be obtained only with the discussed constraints.

Both MNDO and AM1 methods are thus entirely inadequate for the description of the potential energy surface of dilithioacetaldoxime: Several structures that correspond to minima on the ab initio surface do not exist as stationary points on the MNDO surface (and vice versa) and some of the stationary structures that do exist on both surfaces differ in their character.

**Implications for Reaction Mechanisms.** The ab initio results presented account for the higher stability of the syn-configured dimetalated oxime. The characteristics of the structures furthermore account for the preferential deprotonation at the syn  $\alpha$ -carbon and the regioselective addition of electrophiles. These results, however, must be placed in a context of kinetic effects and aggregation.

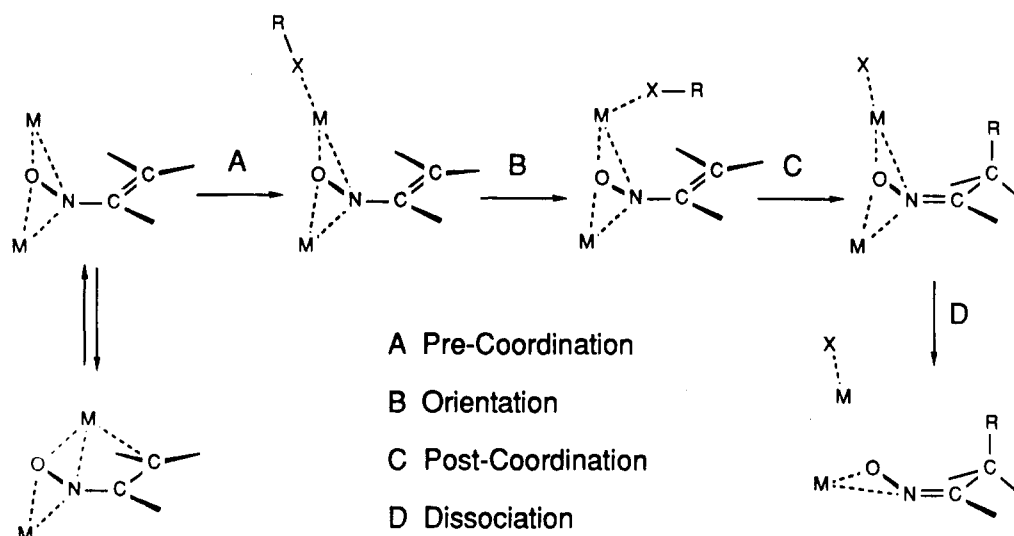
In experimental practice the deprotonations are often carried out under kinetically controlled conditions in which complex-induced proximity effects are important.<sup>54</sup> The theoretical results provide strong evidence for the importance of the chelation of the cations by the heteroatoms. The second deprotonation of an oxime salt<sup>55</sup> is likely to be initiated by precoordination of the base to *both* of the heteroatoms. Such precoordination would place the metalloorganic base close to the syn  $\alpha$ -carbon and in an ideal position for subsequent deprotonation. Moreover, such precoordination would position the metal of the base in a position close to the energetically most favorable structure of the dimetalated oxime to be formed, which should reduce the activation barrier to deprotonation. Deprotonation at the anti  $\alpha$ -carbon would require an energetically less favorable single coordination of the metalloorganic base to nitrogen. In the transition state for the second deprotonation at the anti carbon the topological arrangement of the cations is expected to resemble more a structure of the *anti-D* type (e.g., 9) than the more stable *anti-C* type structure (e.g., 8). The consideration of the possible prereaction scenarios for deprotonation at the syn or the anti  $\alpha$ -carbon and the calculations of the relative stabilities of the isomeric dimetalated products thus provide a straightforward explanation for the preferential syn deprotonation<sup>8</sup> at the molecular level. That is, the precoordination geometries of kinetically determined deprotonations lead to lower transition energies and faster rates because the same features are involved as in the relative energies of the equilibrium structures of the dimetalated products—*kinetic deprotonation leads to the thermodynamically favored products*.

The theoretical study suggests the following mechanism for the addition of an electrophile to the dimetalated oxime (Scheme III). It has been shown that structures of the *syn-C* and of the *syn-D* type are close in energy for the

(54) (a) Beak, P.; Meyers, A. I. *Acc. Chem. Res.* 1986, 19, 356. (b) Meyers, A. I. *Acc. Chem. Res.* 1978, 11, 375. (c) Wakefield, B. J. *Chemistry of Organolithium Compounds*; Pergamon Press: Oxford, 1974.

(55) The lithium salt of acetaldoxime (deprotonation at oxygen) is  $C_s$  symmetric, and lithium coordinates both of the heteroatoms: Glaser, R.; Streitwieser, A., Jr., unpublished results.

Scheme III



lithium and the sodium derivatives of acetaldoxime dianion. Interconversion of the two structures should be rapid since the appropriate vibrational modes have low frequencies. Solvation is likely to favor structures of the type *syn-C* in which both cations are dicoordinated. In structures of type *syn-D*, one cation is effectively tricoordinated and less available for coordination by solvent molecules. In fully solvated *syn-D* the approach of the electrophile to the carbanionic carbon is not impeded. Moreover, the addition of an electrophilic reagent, such as R-X, to the dimetalated oxime presumably involves desolvation and entry of the electrophile into the primary solvent shell of one of the cations as the first elementary step along the reaction pathway. Facile reorganization of the solvent shell then allows the electrophile to approach the reactive carbon. The transition state for the addition of R<sup>+</sup> to the  $\alpha$ -carbon in this fashion should be considerably lower in energy compared to transition states of alternative reaction pathways that proceed without precoordination. In the proposed reaction mechanism the bond formation between the electrophile and the  $\alpha$ -carbon occurs concomitantly to the transfer of the nucleophile X<sup>-</sup> to the coordinated cation. The formation of the salt MX together with the coordination of MX maintained to both of the heteroatoms should lower the activation barrier to such an extent that pathways without such additional stabilization cannot compete.

All of the discussion thus far is based on monomeric species, but the dimetalated oximes discussed in this paper are highly likely to be aggregated in solution.<sup>56</sup> The reactive intermediate could, of course, be the monomer present in small concentration in equilibrium with aggregates, but for dimetalated compounds it seems more likely that the monomer concentration is too small and that it is an aggregate that is the actual reactant. If such is the case, the agreement between theory and experiment indicated above strongly suggests that the reacting dimetalated oxime is not significantly altered by its complexing neighbors within the aggregate and that its chemistry is essentially that of the monomer. A mechanism such as that in Scheme III would be altered by the presence of the complexing neighbors, but the essential features of the

sequence would remain unchanged. That is, this argument implies that the essential reactants are the dianion and its closely bound metal cations and that cooperative interactions between monomers within an aggregate are unimportant.

## Conclusions

The regioselective formation of the *syn*-configured dimetalated oxime derivative is not an intrinsic property of the isomeric dianions. The chiral anti-dianion **2** is energetically favored by 2.2 kcal mol<sup>-1</sup> compared to the planar *syn*-isomer **1**. The preference for **2** is attributed primarily to the strong electrostatic repulsion between the carbanionic center and both of the highly charged heteroatoms in **1**, whereas such repulsion is reduced in the anti-isomer **2**. Electron density analysis provides compelling evidence that through-space homocyclic conjugation of the *syn*-configured dianion, previously considered to favor **1** over **2**, is unimportant.

The calculations of the dimetalated derivatives of acetaldoxime show a *syn* preference in agreement with experiment. Chelation of the dianion is considered to be the dominant factor for the regioselective formation of the metalated enolate equivalents; such structures are clearly important in considerations of reaction mechanism. A *syn*-preference energy of 4.4 kcal mol<sup>-1</sup> has been obtained for dilithioacetaldoxime. Replacement of Li<sup>+</sup> by Na<sup>+</sup> increases the *syn*-preference energy to 8.3 kcal mol<sup>-1</sup> and suggests that a higher degree of regioselectivity may be achieved when organometallic bases with larger cations are used for deprotonation. A similar result has been obtained previously for the effect of the cation on the relative stability of geometrical isomers of metalated oxime ethers.<sup>40,41</sup> The theoretical results indicate that the formation of metalated oximes proceeds with a higher degree of regioselectivity compared to metalated oxime ethers.

Triple ions formed by the heteroatoms and the cations provide the underlying structural concept common to all of the energetically low-lying minima of dimetalated acetaldoxime. Chelation by the heteroatoms is more important than the interaction of the cations with the carbanionic carbon. The lithium triple ions in which one cation is coordinated closely to the carbanionic center and one of the heteroatoms are comparatively high in energy, and such structures do not correspond to local minima. The

(56) Dilithium salts of carboxylic acid are known to be aggregated in tetrahydrofuran: (a) Bauer, W.; Seebach, D. *Helv. Chim. Acta* 1984, 67, 1972. (b) Gronert, S.; Streitwieser, A. *J. Am. Chem. Soc.* 1988, 110, 4418.

triple ions formed between the heteroatoms and the cations differ in detail due to the mode of puckering, and it is these modes of puckering that cause the manifold of topologically different structures in these systems and that ultimately determine the relative energies of the resulting structures. Different triple ion structures differ little in energy and are readily interconverted.

The calculated structures are those for gas-phase monomers; the true species in solution are undoubtedly both solvated and aggregated. Nevertheless, the same fundamental principles identified for the monomeric triple ions probably apply to the aggregates as well; in particular, the observed syn regiochemistry is found for the monomers and does not require any unusual cooperative effects within dimers or higher aggregates. The regioselective syn deprotonation and the regioselective addition of an electro-

phile to the syn  $\alpha$ -carbon appear to be direct consequences of the pronounced trend for the preferential formation of triple ions centered at the heteroatoms.

**Acknowledgment.** This research was supported in part by NSF grants. We thank the San Diego Supercomputer Center and the Campus Computer Facility, UCB, for generous grants of computer time on Cray II and VAX 8800 computers, respectively.

**Supplementary Material Available:** Structures (in *Z*-matrix form), total and relative energies, and vibrational frequencies of structures 1-13 given in Appendix I and structures (in *Z*-matrix form) and heats of formation of structures M1-M8 given in Appendix II (MNDO and AM1) (15 pages). Ordering information is given on any current masthead page.

## Synthesis and Chemistry of Highly Fluorinated Bicyclo[2.2.0]hexenones<sup>1</sup>

Richard R. Soelch, Edward McNierney, Gary A. Tannenbaum, and David M. Lemal\*

Department of Chemistry, Dartmouth College, Hanover, New Hampshire 03755

Received October 4, 1988

A series of highly fluorinated bicyclo[2.2.0]-5-hexen-2-ones (**3**) and their hydrates (**4**) have been prepared in two steps from hexafluoro Dewar benzene (**1**). Photolysis of *exo*-3*H*-pentafluorobicyclo[2.2.0]-5-hexen-2-one (**3d**) at low pressure in the vapor phase gave 1*H*-pentafluorocyclopentadiene (**8**), but in solution the principal product was pentafluorophenol (**9**). Under Favorskii conditions, *exo*-3-bromo- and *exo*-3-chloropentafluorobicyclo[2.2.0]-5-hexen-2-one (**3a** and **3b**) ring opened stereospecifically to 2-cyclobutenecarboxylic acids **17** and **29**, respectively. Treatment of these ketones with *tert*-butoxide under aprotic conditions effected stereospecific cleavage to *tert*-butyl methylenecyclobutenecarboxylates **25** and **30**. The acid (**27**) corresponding to **25** was obtained both from bromohydrate **4a** and the acid **17**, again stereospecifically, by reaction with lithium diisopropylamide. Flash vacuum pyrolysis of the hydrate (**4c**) of hexafluorobicyclo[2.2.0]-5-hexen-2-one at 300 °C gave hexafluoro-2,4-cyclohexadienone (**12**), which decarbonylated at higher temperatures to yield hexafluorocyclopentadiene (**13**). Similarly, flash vacuum pyrolysis of 3-chloropentafluorobicyclo[2.2.0]-5-hexen-2-one (**3b**) at 650 °C gave a mixture of 1- and 2-chloropentafluorocyclopentadienes.

Pentafluorocyclopentadienes bearing hydrogen or halogen at the 5-position are potential sources of the pentafluorocyclopentadienyl ligand, a ligand which holds promise of becoming quite important in organotransition metal chemistry.<sup>2</sup> Prior to our studies, syntheses of pentafluorocyclopentadienes<sup>3</sup> and the perfluoro compound<sup>4</sup> were based on fluorination of appropriate five-membered ring

precursors. Typically, they involved complicated product mixtures and low yields. We were thus led to consider quite different routes to this family of compounds.<sup>5</sup> In particular, we were attracted to hexafluorobenzene as a starting material because it is readily available, relatively inexpensive (for a fluorocarbon), and capable of being photoisomerized easily in excellent yield to the reactive hexafluoro Dewar benzene (**1**).<sup>7,8</sup> As will become clear, our schemes for ring contracting this compound to produce bicyclo[2.1.0]pentenes and their cyclopentadiene valence isomers have gone awry, for the most part. Nonetheless, they have led to unusual chemistry, to examples of remarkable stereoelectronic control, and to a family of highly

(1) This paper is based principally on the Ph.D. Dissertation of R. R. Soelch, Dartmouth College, 1984.

(2) High promise is suggested by (1) the ubiquity of the cyclopentadienyl ligand in organotransition metal chemistry, (2) the striking changes in reactivity of its complexes which substitution on that ligand can produce (cf. pentamethylcyclopentadienylmetal chemistry), and (3) the fact that other perfluorinated ligands form a wealth of stable complexes with transition metals.

(3) (a) Banks, R. E.; Bridge, M.; Haszeldine, R. N.; Roberts, D. W.; Tucker, N. I. *J. Chem. Soc. C* 1970, 2531-2535. (b) Fields, R.; Green, M.; Harrison, T.; Haszeldine, R. N.; Jones, A.; Lever, A. B. P. *J. Chem. Soc. A* 1970, 49-58. Bergomi, A.; Burdon, J.; Tatlow, J. C. *Tetrahedron* 1966, 2551-2554.

(4) Banks, R. E.; Bridge, M.; Haszeldine, R. N. *J. Chem. Soc. C* 1970, 48-49 and references therein. Moore, E. P., U.S. Patent No. 3,686,336, 1972; *Chem. Abstr.* 1973, 78, P3832u. Harris, J. F., Jr.; U.S. Patent No. 3,449,304, 1969. Burdon, J.; Hodgins, T. M.; Perry, D. R. A.; Stephens, R.; Tatlow, J. C. *J. Chem. Soc.* 1965, 808-810.

(5) In addition to the routes described in this paper, we have developed other pathways to some of these highly fluorinated cyclopentadienes.<sup>6</sup>

(6) (a) Soelch, R. R.; Mauer, G. W.; Lemal, D. M. *J. Org. Chem.* 1985, 50, 5845-5852. (b) Unpublished work by these authors.

(7) Camaggi, G.; Gozzo, F.; Cevdalli, G. *J. Chem. Soc., Chem. Commun.* 1966, 313. Haller, I. *J. Am. Chem. Soc.* 1966, 88, 2070.

(8) Sixty percent conversion of the benzene to its Dewar isomer has been reported, but we have found that longer irradiation times increase the conversion (and yield) to about 90%.